Inelastic Neutron Scattering Study of Hydrogen-Bonded Solid Formamide at 15 K

Cheok N. Tam,*,† Petr Bour,‡ Juergen Eckert,§ and Frans R. Trouw†

Intense Pulsed Neutron Source Division, Argonne National Laboratory, Building 360, 9700 South Cass Avenue, Argonne, Illinois 60439; Institute of Organic Chemistry and Biochemistry, Academy of Sciences of the Czech Republic, Flemingovo nam 2, 16610 Prague, Czech Republic; and LANSCE, Los Alamos National Laboratory, Mail Stop H805, Los Alamos, New Mexico 87545

Received: January 8, 1997; In Final Form: May 23, 1997[⊗]

The inelastic neutron scattering spectra for formamide ($HCONH_2$) and its N-deuterated isomer ($HCOND_2$) have been measured. The spectra are interpreted on the basis of a vibrational harmonic normal-mode analysis using a variety of models. The models are a single molecule, a formamide dimer, a tetramer resembling the unit cell of crystalline formamide, and a cluster of 36 formamide molecules. Force fields of the first three model systems were computed ab initio using the B3LYP DFT functional and the 6-31G** basis set. The tetramer force field was then applied to the cluster of 36 molecules. Most of the observed vibrational bands could be assigned by comparing the relative INS intensities and frequencies calculated for the theoretical models with the measured spectra. Reasonable agreement between the calculation and the experiment was achieved on this basis. The results confirm the presence of the strong hydrogen bonding in the formamide lattice. However, the previously proposed model for the hydrogen bonding in *N*-methylacetamide involving a dynamical proton exchange between the amidic (···OCNH···) and imidolic (···HOCN···) forms is not consistent with our findings.

Introduction

Formamide is one of the simplest compounds that exhibit hydrogen bonding between amide groups. This type of hydrogen bond, present in many polymer systems such as polypeptides, proteins, and polyamides, plays a key role in their secondary structure and reactivity, and hence their biological function.[1] Many questions remain about the degree of the electron delocalization (charge transfer) accompanying the formation of hydrogen-bonded amide group clusters.

Vibrational spectroscopy has been extensively used to investigate the details of the structures and interactions in polypeptides and proteins.[2] Since the classic study by Miyazawa and co-workers,[3] a tremendous amount of work has been done on biorelated molecules using IR and Raman spectroscopy.[4] Nevertheless, the low-frequency region, which is of interest for slow biological processes, is not easily accessible by conventional optical techniques. Inelastic neutron scattering (INS) spectroscopy is an attractive option in the low-frequency regime. In addition, due to the high incoherent neutron scattering cross section for hydrogen and the vibrational amplitude weighting of the intensity of the scattering, the INS technique has a preferential sensitivity for proton movements. This makes INS a very useful technique for studies of hydrogen-bonded systems. Recent results are very encouraging with respect to the understanding of the hydrogen bonding in simple amide systems and peptides.[5] Also, the spectral broadening in IR and Raman spectroscopy caused by extensive intermolecular hydrogen bonding is absent in INS because neutrons interact only with the nuclei. Furthermore, INS spectroscopy of oriented samples can potentially provide a great deal of detailed information on the character of vibrational modes.[6]

It has been recognized previously that many vibrational frequencies in the amide group are shifted by the formation of hydrogen bonds.[7] For example, the N−H stretching frequencies are reduced by about 100 cm^{-1}, while the frequency of the out-of-plane distortion modes generally increases. It is possible to relate the N−H stretching frequencies to the N−O distance in such systems[7] and generally to the strength of the hydrogen bond. Recently, based on the INS data of solid *N*-methylacetamide, a model has been proposed suggesting a double-minimum potential for the hydrogen in bonded amides and peptides.[5] Naturally, this would lead to the formation of a resonance structure of the amidic (···OCNH···) and imidolic (···HOCN···) forms of the hydrogen-bonded molecules or to a dynamical proton exchange between them. As an alternative definition, the hydrogen bond becomes ionic ($N^{\delta-}\cdots H^{\delta+}\cdots O^{\delta-}$). Such a model implies a long-distance cooperativity during the formation of the hydrogen bonds because of the chaining of the molecules. Yet according to other studies[7,8] the hydrogen bonding does not disturb substantially the formamide molecule, and the ionic character of the bond cannot be compared to the truly ionic interactions in inorganic crystals.[6]

In this study, crystalline formamide is modeled on the basis of computationally tractable clusters. The single-minimum harmonic potential obtained by an ab initio method for these smaller systems is then compared with the experimental INS spectra. Similar studies have been conducted previously using empirical potentials.[9] The empirical methods cannot be used systematically, and they lack the flexibility needed for a more complex model. Ab initio techniques generally provide more reliable and accurate force fields, although their power is still limited by the computational requirements of such approaches. A recently introduced so-called hybrid DFT/HF functional has been shown to be a useful tool for vibrational studies on smaller molecules.[8,10−15] More recently, the DFT force-field calculations on formamide monomer and dimers have been published.[8,15] These calculations are extended to a tetramer and a large 36-molecule cluster with the aim of simulating the experimental INS spectra. Moreover, the effect of the anharmonic forces on spectral intensities are estimated for the monomer and dimer. On the basis of these models, the

* To whom correspondence should be addressed.
† Argonne National Laboratory.
‡ Academy of Sciences of the Czech Republic.
§ Los Alamos National Laboratory.
⊗ Abstract published in *Advance ACS Abstracts,* August 1, 1997.

S1089-5639(97)00122-9 CCC: $14.00

experimental vibrational bands can be assigned and classified. Furthermore, the effect of hydrogen bonding on the geometry, vibrational frequencies, and INS intensities is determined.

Experimental Section

Formamide ($HCONH_2$) was purchased from Aldrich and used without further purification. The N-deuterated formamide ($HCOND_2$) was synthesized from $HCONH_2$ by successive isotopic substitution using D_2O (Aldrich). The resulting N-deuterated formamide sample was analyzed by NMR and was shown to be ~90% N-deuterated.

The INS spectra were recorded using the CHEX inelastic neutron spectrometer at the Intense Pulsed Neutron Source (IPNS) located at Argonne National Laboratory. The CHEX spectrometer utilizes a fixed final energy, with the time-correlation of the pulsed source providing the energy-transfer determination. The scattered neutron beam is reflected by an analyzer crystal array (highly oriented pyrolytic graphite) and only neutrons with specific wavelengths (satisfying the Bragg condition) will be reflected and detected. In addition, a beryllium filter is placed between the analyzer crystal and the detectors to reject the higher order reflections, thereby removing any ambiguity in the final energy of the detected neutrons. The spectrometer incorporates a time focusing design to achieve an energy resolution ($\Delta\nu/\nu$) of <2% for frequencies below 2000 cm^{-1}. The samples were placed in an "organ pipe"-like cell which consists of a row of vertical small aluminum tubes covering the whole cross section of the incident neutron beam (10 × 10 cm). The whole sample assembly was cooled to 15 K. The raw time-of-flight INS data were converted to neutron energy loss data by standard procedures developed at IPNS.

A similar INS measurement of crystalline formamide has also been carried out at the Los Alamos National Laboratory using the FDS instrument at the Manuel Lujan Jr. Neutron Scattering Center. The INS spectra produced by both neutron facilities are in close agreement, and only the INS spectra from IPNS are used here because the CHEX spectrometer has a better energy resolution.

Computational Methods

The formamide monomer (FA), dimer (FA2), and tetramer (FA4) were modeled using the same computational procedure. The geometry of the clusters was optimized by energy minimization, at the B3LYP/6-31G** level.[12] Gaussian 94[16] was used for the calculation, as implemented at the Supercomputer Center of the Charles University in Prague, Czech Republic. The geometries of the molecular systems are shown in Figure 1. The dimer (tetramer) structure was chosen to resemble part (whole) of the crystal unit cell. In accordance with the neutron diffraction data,[17] the C_s (for FA) and C_{2h} (for FA2 and FA4) symmetry were employed to speed up the calculations. After optimization, the harmonic force fields were calculated at the same level by Gaussian 94, using the analytic derivative technique. These force fields calculations are done in the Cartesian coordinate system instead of using a set of defined internal coordinates, to facilitate the transfer of the force field to larger clusters.[18]

Similarly, the large 36-molecule cluster (FA36) was optimized using the PM3 semiempirical Hamiltonian with Gaussian 94. The starting geometry was chosen to resemble the crystal structure, implementing the C_{2h} symmetry (see Figure 1). Then the tetramer DFT force field was transferred onto the cluster in the Cartesian coordinate system,[18] in an effort to obtain the main terms of the FA36 force field.

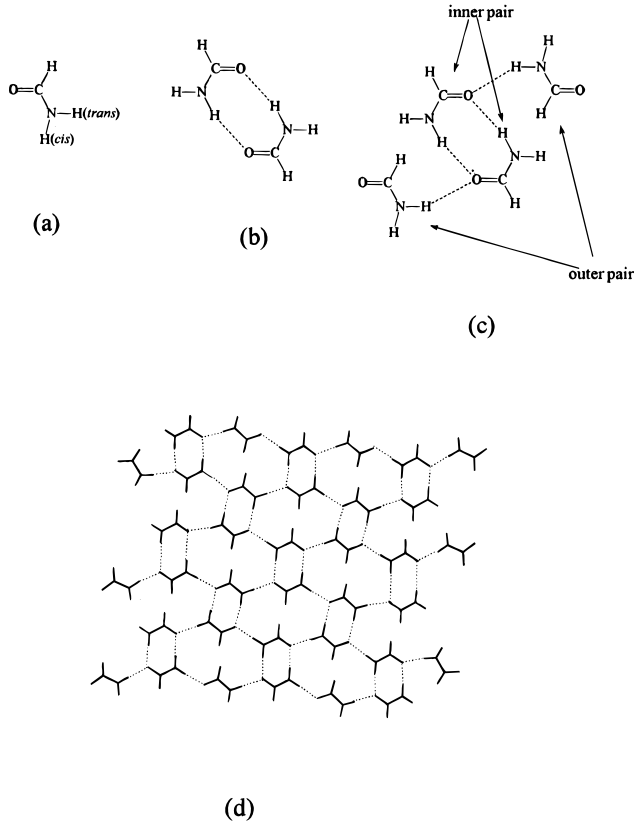

Figure 1. Molecular models of formamide: (a) monomer, (b) dimer, (c) tetramer, and (d) the 36-molecule cluster. Note that all the model systems are planar. The FA models are assembled according to the structure of the FA unit cell from ref 17. The dotted lines indicate the hydrogen bonds.

The normal-mode atomic displacements (after isotopic substitution for the deuterated species) were calculated. The INS intensity for each vibrational mode is approximately proportional to the sum of the mean-square displacements of the protons attributable to the vibrational mode. The CHEX spectrometer measures INS intensities with a parabolic cut through the momentum transfer space. Our program for generating INS intensities takes into account this momentum transfer weighting effect. An empirical method adopted from ref 19 were used for the intensity calculation. The relative INS intensities, S_k, can be approximately expressed as

$$S_k = {}^1/_3 c\nu_k \exp(-c\alpha\nu_k)\sum_i^N \sigma_i C_{ik}^{\ 2} \qquad (1)$$

where c is a convenience factor (c = 1/16.132), ν_k is the transition frequency in cm^{-1}, σ_i is the incoherent scattering cross section taken from ref 20, and C_{ik} is the mass-weighted eigenvector of atom i. The parameter, α, controls the total Debye−Waller factor. If the phonon wings, combinations and overtone bands are ignored, α is the sum of the isotropic internal-mode temperature factor, U_v, and the external-mode temperature factor, U_e.[19] U_v governs the intensity falloff for the total internal-mode intensity, while U_e governs the distribution of the total internal-mode intensity between the parent internal mode and the phonon wings.[19] U_v calculated from the mass-weighted eigenvector is about 0.04 $Å^2$ for all of the hydrogen atoms in formamide. As the experimental data yield a value for α of 0.06 $Å^2$, U_e is estimated to be 0.02 $Å^2$. This approach is sufficient to achieve our goal of assigning the internal modes, which does not require a detailed fit of the INS profile.

TABLE 1: Geometry of the FA Model Systems[a]

model	R(N−H) trans/cis[b]	R(C−H)	R(C═O)	R(C−N)	R(N···O)
FA, DFT	1.007/1.010	1.010	1.216	1.362	
FA, PM3	0.990/0.992	1.101	1.220	1.391	
FA2	1.029/1.008	1.106	1.232	1.342	2.874
FA4 (IP)[c]	1.008/1.027	1.111	1.239	1.336	2.899 (cyclic)
FA4 (OP)[c]	1.016/1.009	1.111	1.219	1.353	2.986 (zigzag)
FA36, PM3 inner[d]	1.006/1.010	1.108	1.224	1.362	2.821 (cyclic)
FA36, PM3 outer[d]	1.007/1.010	1.110	1.245	1.361	2.812 (zigzag)
experiment					
gas phase[e]	1.027(6)/1.027(6)	1.125(12)	1.212(3)	1.368(3)	
solid state[f]	1.048(6)	1.096(6)	1.239(7)	1.294(5)	2.958(7) (cyclic)
				1.326(4)[g]	2.853(7) (zigzag)

[a] Bond lengths given in Å, R(N··O) is the hydrogen bond length. [b] trans/cis indicates the N−H bond length for the N-hydrogen trans or cis to the oxygen within the same molecule. This is also indicated in Figure 1. [c] IP and OP are the inner and outer pairs indicated in Figure 1. [d] Outer FA are the ones which are at the edges of the unit cells and only one N−H atom/FA molecule is H-bonded. Inner FA are the ones which are located inside the clusters with both N−H atoms in the FA molecules are H-bonded. [e] Gas electron diffraction.[23] [f] Neutron diffraction, 7 K.[17] [g] X-ray diffraction.[22]

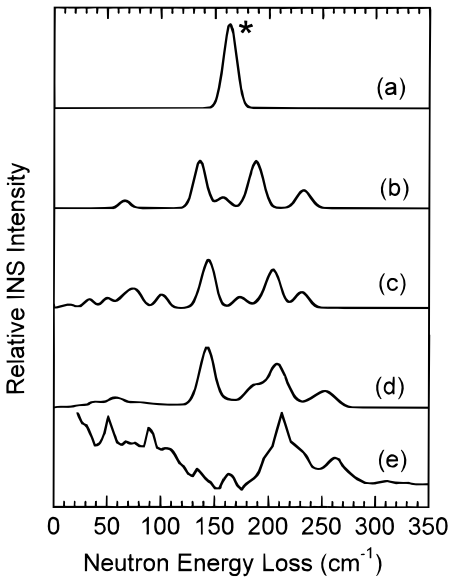

Figure 2. Simulated INS spectra of formamide ($HCONH_2$): (a) the monomer, (b) the dimer, (c) the tetramer model, (d) the FA36 model, and (e) experimental spectrum in the range 0−350 cm^{-1} (the asterisk indicates the NH_2 wagging mode in the monomer).

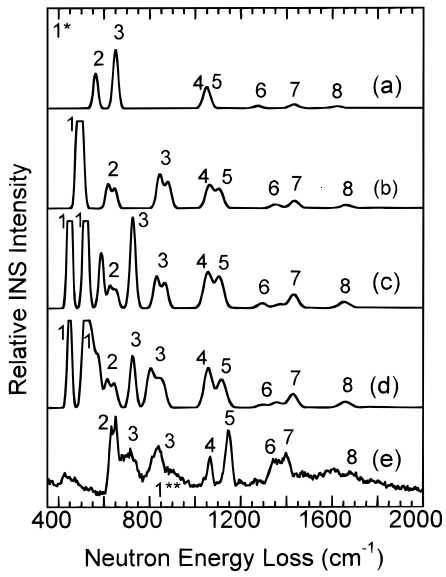

Figure 3. Simulated INS spectra of formamide ($HCONH_2$): (a) the monomer, (b) the dimer, (c) the tetramer model, (d) the FA36 model, and (e) experimental spectrum in the range 350−2000 cm^{-1} (the asterisk indicates the NH_2 wagging mode in the monomer, (the double asterisk indicates the NH_2 wagging frequency suggested by the IR data at 20 K from ref 25). The predicted and experimental INS features are correlated by the numbers: (1) NH_2 wagging; (2) NCO bend + C−N stretch + NH_2 rocking; (3) NH_2 torsion; (4) C−H wagging; (5) NH_2 rocking; (6) amide III (N−H bend + C−N stretch); (7) C−H bend; (8) amide II (N−H bend + C−N stretch).

To estimate anharmonic effects, a procedure similar to that of ref 21 was used. This could be carried out only for the monomer and the dimer due to computational limitations. The third and semidiagonal (d_{ijkl} with four different indices excluded) fourth Cartesian energy derivatives were calculated by numerical differentiation, using the Gaussian 94 program. For FA, the B3LYP/6-31G level was again used for the calculation of second derivatives with a differentiation step size of 0.1 Å. For FA2, the HF/6-31G** level was used with a step size of 0.01 Å (such a small step would lead to a numerical instability for the DFT grid-based methods).

The theoretical INS profiles were simulated from the calculated INS intensities using the Gaussian instrumental energy resolution function for all transitions. The simulated resolution function was assumed to increase linearly with frequency, and the proportionality constant was chosen to mimic the observed experimental widths.

Results

Geometry. Selected geometry parameters are given in Table 1 for the model systems, and compared with the experimental parameters for the monomer and crystalline formamide. The monomer structure is not dramatically perturbed by the electron conjugation in the crystal, where the bond lengths differ by about 1−2%. There is evidence of electron rearrangement toward the imido form of the molecule as the hydrogen bonding takes place in the clusters. The N−H distance, for example, lengthens as the hydrogen bonds to the oxygen and the calculated N−H bond length increases by 0.017 Å for the H-bonded N−H(cis to the oxygen within the same molecule) of the inner pair of FA4 (the structure which is closer to an infinite crystal) as compared to the N−H(cis) distance of the FA/DFT monomer. This compares favorably with the experimentally observed increase of 0.021 Å (comparison of the gas-phase and solid-phase structures). The same comparison of the FA/DFT and the inner pair of the FA4 models indicates that the C═O bond length increases by 0.023 Å, which is also close to the experimental difference in C═O bond length (between those in the gas and solid phases) of 0.027 Å. The calculated bond length of the C−N bond is 0.026 Å shorter in the inner pair of FA4 than for the FA/DFT monomer, which is in relatively poor

TABLE 2: Vibrational Frequencies (in cm^{-1}) of Formamide

mode[a]	FA	FA2	FA4	expt (INS)	expt (Raman/IR)[c]	assignment for FA4[d]
1	3740 A′[b]	3686 Bu[b]	3690 Ag[b]			asym N−H stretch, OP
2			3690 Bu			asym N−H stretch, OP
3		3685 Ag	3683 Ag		3265	asym N−H stretch, IP
4			3683 Bu			asym N−H stretch, IP
5	3596 A′	3325 Bu	3504 Bu			sym N−H stretch, OP
6			3504 Ag			sym N−H stretch, OP
7		3269 Ag	3357 Bu		3217	sym N−H stretch, IP
8			3310 Ag		3124	sym N−H stretch, IP
9	2951 A′	2986 Ag	3026 Ag		2893	C−H stretch, IP
10			3023 Bu			C−H stretch, IP
11		2982 Bu	2915 Bu			C−H stretch, OP
12			2915 Ag			C−H stretch, OP
13	1835 A′	1812 Bu	1834 Ag			C═O stretch (amide I), OP
14			1834 Bu			C═O stretch, OP
15		1780 Ag	1797 Bu		1748	C═O stretch, IP
16			1765 Ag			C═O stretch, IP
17	1620 A′	1664 Bu	1660 Bu	1697	1692	amide II (N−H bend + C−N stretch), IP
18			1659 Ag			amide II, IP
19		1661 Ag	1651 Bu	1623		amide II, OP
20			1648 Ag			amide II, OP
21	1432 A′	1435 Bu	1433 Ag	1405	1396	C−H bend
22			1432 Bu		1373	C−H bend
23		1435 Ag	1432 Ag			C−H bend
24			1432 Bu			C−H bend
25	1275 A′	1362 Ag	1376 Ag	1363	1358	amide III (N−H bend + C−N stretch), IP
26			1360 Bu			amide III, IP
27		1344 Bu	1294 Bu			amide III, OP
28			1293 Ag			amide III, OP
29	1054 A′	1111 Ag	1119 Ag	1153	1154	NH_2 rocking, IP
30			1109 Bu		1143	NH_2 rocking, IP
31		1102 Bu	1102 Ag			NH_2 rocking, OP
32			1102 Bu			NH_2 rocking, OP
33	1046 A″	1069 Au	1071 Au	1073	1061	C−H wagging, IP
34			1061 Bg			C−H wagging, IP
35		1056 Bg	1047 Bg			C−H wagging, OP
36			1047 Au			C−H wagging, OP
37		881 Au	868 Au	843		NH_2 torsion, IP
38			831 Bg			NH_2 torsion, IP
39	650 A″	844 Bg	727 Au	721		NH_2 torsion, OP
40			726 Bg			NH_2 torsion, OP
41	563 A′	648 Bu	653 Bu	686	676	NCO bend + C−N stretch + NH_2 rocking, IP
42			626 Ag	657	646	NCO bend + C−N stretch + NH_2 rocking, IP
43		618 Ag	589 Bu		641	NCO bend + C−N stretch + NH_2 rocking, OP
44			587 Ag		619	NCO bend + C−N stretch + NH_2 rocking, OP
45	126 A″	503 Bg	523 Bg		841	NH_2 wagging, IP
46			516 Au			NH_2 wagging, IP
47		485 Au	450 Bg			NH_2 wagging, OP
48			449 Au			NH_2 wagging, OP
49			231 Bu	264	262,231	FA rotation, IP
50		189 Bg	205 Bg	213	224	FA rotation, IP
51		183 Ag	194 Ag			FA rotation, IP+OP
52		158 Ag	174 Ag		178,171	FA translation, IP
53		136 Au	145 Au	166	146	FA rotation, IP
54			138 Bu		128	FA trans + rotation, OP
55			101 Ag		92	FA translation + rotation, OP

[a] The lower energy modes (<100 cm^{-1}) of the FA tetramer model cannot be assigned due to the interferences from the phonon density of states in the experimental spectrum. Thus, the number of normal modes shown in this table for the FA tetramer is less than ($3N - 6$). [b] Symmetry species of the vibrational modes. [c] Raman/IR data measured at 20 K are taken from ref 25. [d] Abbreviations: OP/IP − inner/outer pair in FA4, as indicated in Figure 1.

agreement with the difference of 0.042 Å observed experimentally (comparison of the X-ray[22] and gas electron diffraction[23] values). The C−N bond length of 1.294 Å obtained by neutron diffraction indicates a shortening of 0.074 Å upon crystallization. In contrast, an X-ray study gave a C−N bond length of 1.326 Å. Our calculation is in better agreement with the X-ray result. The C−H bond length increases by less than 0.2% according to the calculations, which is consistent with the experiments. The N···O distance is longer in the tetramer than in the dimer, which would suggest that the "H-binding ability" is essentially saturated in the dimer. In a real crystal, the alternating H-bond lengths are shorter than for the cyclic ones, which is predicted by previous calculations[24] and by our PM3 model taking into account the long-range electron conjugation, unlike the DFT calculation on the tetramer. A detailed study of this long-range electron transfer or conjugation at a reliable level is currently beyond our computational possibilities.

INS Spectra for Formamide. The theoretical and experimental spectra are shown in Figures 2 and 3. Due to the lower spectral resolution at higher frequencies, in combination with the weaker scattering intensities, the C−H and N−H stretching bands over 2000 cm^{-1} are poorly defined. For the purpose of the mode assignment, those high-frequency modes are of limited utility. On the other hand, the signals of the lower frequency

modes are relatively intense, and the comparison between experiment and theory will focus on this region.

The mode assignments and frequencies are given in Table 2, where the INS derived vibrational frequencies are also compared with those from a Raman/IR study at 20 K.[25] There is remarkable agreement between the two different techniques at frequencies below 1700 cm^{-1}. The Raman/IR data also provide a basis for a comparison of our theoretical results with experiment.

The theoretical calculations overestimate the frequency of the N−H stretch by more than 150 cm^{-1}. This may partly be due to the fact that not all the N−H are H-bonded in the models. Furthermore, the calculations also overestimate the frequencies of the C−H and C═O stretches by about 100 cm^{-1}. This is not surprising because, in general, Hartree−Fock and even DFT methods do not include, or inadequately account for, electron correlation.[12,15] This is of less concern for lower frequency vibrational modes.[12]

The single FA molecule simulated spectrum provides an indication of the expected intensity as a function of frequency. As the cluster size grows from FA to FA4, the low-energy modes, corresponding to the translational and rotational motions of formamide molecules within the clusters, are located in the 0−350 cm^{-1} region, as shown in Figure 2. Unfortunately, the experimental spectrum in this region contains a contribution from the phonon density of states, which is difficult to model within the framework of the theoretical approach used in this paper. However, the peaks between 150 and 270 cm^{-1} in the experimental spectrum compare well with the FA4 and FA36 models. As is apparent from Table 2, the relative translational and rotational motions between the FA molecules within the lattice can be related to the observed bands in this low-frequency region.

The NH_2 wagging frequency increases from 126 cm^{-1} for the monomer to ∼500 cm^{-1} for the dimer and tetramer, under the influence of the H-bonding. For the FA4 model, the stronger bands of the out-of-plane NH_2 wagging motions occur in the range 450−525 cm^{-1}, but the vibrational amplitudes for these motions contain contributions from the large-amplitude motions of the non-H-bonded "free" hydrogens. These large-amplitude motions do not exist in a real crystal, and these intense peaks will not be observed in the experiment. Instead, the NH_2 wagging peak should be considerably weaker as the amide groups which are H-bonded will have lower vibrational amplitudes. The low-temperature IR data indicate that the N−H wagging frequency is 841 cm^{-1}.[25]

The signals between 550 and 2000 cm^{-1} can be compared with experiment on the basis of calculated frequencies and intensities. As shown in Figure 3, the NCO bend + C−N stretch + NH_2 rocking mode and the NH_2 torsion mode are correctly predicted by the FA4 and FA36 models. Modes in the 1000−1120 cm^{-1} region involve the hydrogens of the NH_2 group, as well as the motion of the C hydrogens. The signal of the C−H out-of-plane wagging (∼1050 cm^{-1} experimentally) is predicted to be approximately of the same intensity as that of the N−H in-plane motion (∼1100 cm^{-1}, experimentally 1121 cm^{-1}) whereas the latter mode is about twice as intense as the former in the experimental INS spectrum. The higher predicted INS intensity for the C−H out-of-plane motion arises from the relatively unrestricted wagging due to the lack of the interactions between the crystal unit planes. The predicted frequencies and intensities of the C−H in-plane bending and the amide II and the amide III modes are well correlated with the experimental spectrum. The spectrum of FA36 retains the basic features observed in the spectrum of the tetramer, but the overall shape becomes more realistic; namely, the signal from the formamide molecules at the edge of the cluster is weaker (in FA4 there are four non-H-bonded hydrogens and four H-bonded ones, in FA36, the ratio is 16:56).

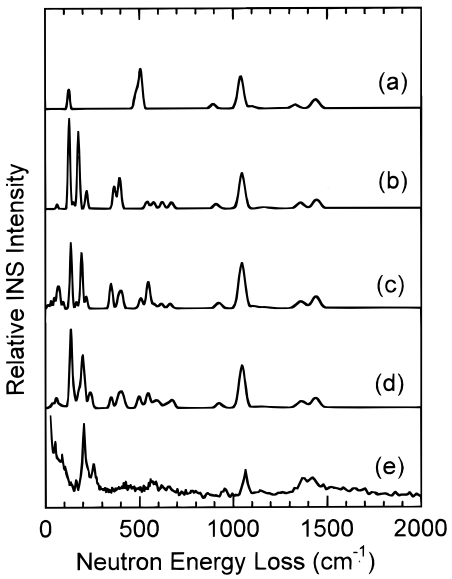

Figure 4. Simulated INS spectra of N-deuterated formamide ($HCOND_2$): (a) the monomer, (b) the dimer, (c) the tetramer model, (d) the FA36 model, and (e) the experimental spectrum in the range 0−2000 cm^{-1}.

Effect of Deuteration. The simulated and experimental spectra for the N-deuterated isomer are given in Figure 4, and the corresponding vibrational band assignments are listed in Table 3. From the FA4 model, similar spectral features are predicted in the low-energy region (0−350 cm^{-1}) as for the hydrogenated case, which is in accordance with the experimental observation. The signal of the "free" deuterium wagging (350−400 cm^{-1}) is again not seen experimentally. It should be noted that the frequency of this mode is substantially shifted compared to that for the free FA molecule. We therefore expect that the anharmonic effects will be much smaller in the crystal force field than in the single-molecule force field.[26] The overall gradual decrease in intensity in the region 200−900 cm^{-1} is in accordance with experiment. The effect of the isotopic substitution can be observed for the bands corresponding to the ND_2 and CH motions. The ND_2 in-plane rocking mode frequency is lowered (to 930 cm^{-1}, experimentally 933 cm^{-1}) and the relative mode ordering for the ND_2 in-plane and C−H out-of-plane wagging modes is reversed, as the frequencies of the latter are practically unchanged by the deuteration (1045 cm^{-1}, experimentally 1042 cm^{-1}). Since the incoherent scattering cross section of hydrogen is larger than that of deuterium by about a factor of 16, this means that the C−H out-of-plane motions are dominant in this region. Also, the relative intensity of the ND_2 in-plane mode signal drops to about one-fifth of that of the C−H out-of-plane modes, which is in accordance with the experimental observation. Generally, the simulated spectra for the N-deuterated compounds are in better accord with experiment than is the case for undeuterated formamide.

The INS spectrum of C-deuterated formamide ($DCONH_2$) can be obtained by the subtraction of the INS spectrum of $HCOND_2$ from $HCONH_2$. There will be small differences between the spectrum obtained in this manner and the actual INS spectrum for this compound, but they are of no consequence when assigning the modes. Figure 5 shows INS spectrum of $DCONH_2$ calculated by this method.

Anharmonic Effects. As the force field of formamide is expected to be strongly affected by the anharmonic interactions,

TABLE 3: Vibrational Frequencies of $HCOND_2$[a]

mode	FA	FA2	FA4	expt (INS)	assignment
1	2951 A′	2986 Ag	3026 Ag		C−H stretch, IP
2			3025 Bu		C−H stretch, IP
3		2984 Bu	2915 Bu		C−H stretch, OP
4			2915 Ag		C−H stretch, OP
5	2771 A′	2714 Ag	2731 Ag		asym N−D stretch, OP
6			2730 Bu		asym N−D stretch, OP
7		2714 Bu	2715 Ag		asym N−D stretch, IP
8			2714 Bu		asym N−D stretch, IP
9	2596 A′	2428 Bu	2538 Bu		sym N−D stretch, OP
10			2538 Ag		sym N−D stretch, OP
11		2388 Ag	2449 Bu		sym N−D stretch, IP
12			2415 Ag		sym N−D stretch, IP
13	1829 A′	1800 Bu	1826 Ag		C═O stretch, OP
14			1825 Bu		C═O stretch, OP
15		1749 Ag	1782 Bu		C═O stretch, IP
16			1733 Ag		C═O stretch, IP
17	1440 A′	1467 Ag	1446 Ag	1407	C−H bend, IP
18			1444 Bu		C−H bend, IP
19		1446 Bu	1440 Ag		C−H bend, OP
20			1440 Bu		C−H bend, OP
21	1332 A′	1361 Bu	1373 Bu		amide II, IP
22			1371 Ag		amide II, IP
23		1359 Ag	1349 Bu		amide II, OP
24			1347 Ag		amide II, OP
25	1103 A′	1184 Ag	1185 Ag		amide III, IP
26			1158 Bu		amide III, IP
27		1155 Bu	1115 Ag		amide III, OP
28			1115 Bu		amide III, OP
29	1043 A″	1051 Au	1056 Au	1073	C−H wagging, IP
30			1052 Bg		C−H wagging, IP
31		1048 Bg	1042 Au		C−H wagging, OP
32			1042 Bg		C−H wagging, OP
33	896 A′	914 Ag	930 Bu	961	ND_2 rocking, OP
34			930 Ag		ND_2 rocking, OP
35		909 Bu	922 Ag		ND_2 rocking, IP
36			916 Bu		ND_2 rocking, IP
37	507 A″	672 Au	664 Au		ND_2 torsion, IP
38		623 Bg	617 Bg		ND_2 torsion, IP
39	484 A′	576 Bu	579 Bu		NCO bend + C−N stretch + ND_2 rocking, IP
40		541 Ag	549 Ag		NCO bend + C−N stretch + ND_2 rocking, IP
41			547 Au	562	ND_2 torsion, OP
42			547 Bg		ND_2 torsion, OP
43			508 Bu		NCO bend + C−N stretch + ND_2 rocking, OP
44			507 Ag		NCO bend + C−N stretch + ND_2 rocking, OP
45	126 A″	395 Bg	405 Bg		ND_2 wagging, IP
46		367 Au	389 Au		ND_2 wagging, IP
47			349 Au		ND_2 wagging, OP
48			349 Bg		ND_2 wagging, OP
49		219 Bu	217 Bu	255	FA rotation, IP
50		127 Au	193 Au	205	FA rotation, IP
51		180 Ag	190 Ag		FA rotation/translation
52		150 Ag	166 Ag		FA translation, IP
53		177 Bg	137 Bg	160	FA rotation, IP
54			131 Bu		FA translation, OP
55			95 Ag		FA rotation, OP

[a] Symbols and units same as in Table 2.

an attempt was made to determine the effect of an anharmonic force field on the predicted INS intensities. Figure 6 shows the effect of anharmonicity on the predicted spectrum. For the monomer, the inclusion of anharmonicity leads to extra bands, corresponding to overtone and combination transitions. However, assignment of the extra bands to features in the experimental spectra is difficult. Extra bands appear also in the anharmonic spectrum of the dimer. Here the lowest-frequency modes ($0-350\ cm^{-1}$) spread out over a wider frequency region; they look quite realistic when compared to the measured spectrum, although any detailed agreement is not possible without taking account of the lattice phonon density of states. In the region above $550\ cm^{-1}$ many combination transitions appear, which is consistent with the rather unresolved experimental pattern. A detailed assignment of these modes is clearly impossible. Due to the limited vibrational basis set, which is unavoidable with our current computational constraints, the accuracy of the calculated anharmonic force field is limited. This precludes a quantitative comparison, but it is certainly the case that the anharmonic effects contribute substantially to the intensity pattern, and the intensity changes are comparable with those caused by the H-bond formation.

Discussion

The results of this study demonstrate that we can interpret the basic features of the experimental INS spectra using an ab initio force field based on small clusters of formamide. This approach can explain, for example, the increase in the NH_2 bending frequency, and the decrease in the NH_2 stretching

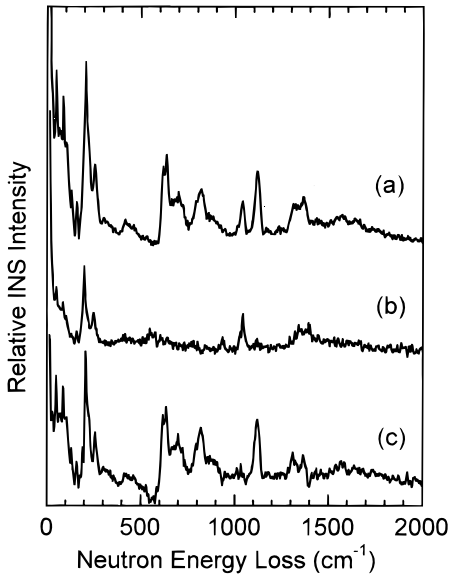

Figure 5. (a) Experimental INS spectrum of formamide ($HCONH_2$); (b) experimental INS spectrum of N-deuterated formamide ($HCOND_2$); (c) INS spectrum of C-deuterated formamide ($DCONH_2$) obtained from the subtraction: INS($HCONH_2$)−INS($HCOND_2$).

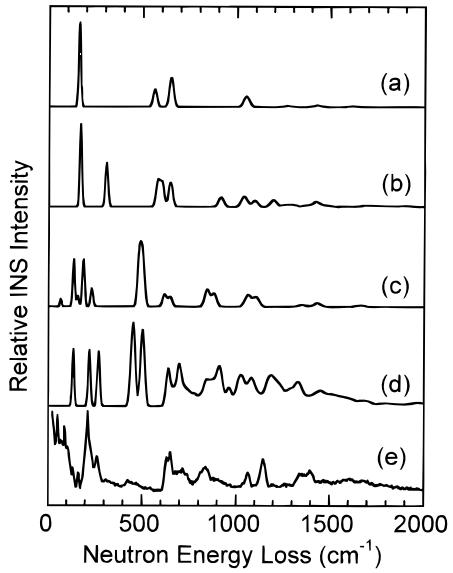

Figure 6. Simulated INS spectra with anharmonic corrections: (a) harmonic monomer, (b) anharmonic monomer, (c) harmonic dimer, (d) anharmonic dimer, and (e) the experimental spectrum.

frequency due to the formation of intermolecular hydrogen bonds. Detailed experimental studies of this effect have been done using IR spectroscopy, on the solvent and concentration dependence of the out-of-plane N−H bending frequency of *N*-methylacetamide (NMA).[27] Fillaux et al. showed that the N−H bending frequency decreases from 725 to 418 cm^{-1} on going from pure liquid to dilute solution in cyclopentane.[27] Another similar IR study on a cyclic amide, 5-methylpyrrolidinone demonstrated that the N−H stretching frequency increases from 3237 to 3443 cm^{-1} on going from neat liquid to dilute solution in deuterated chloroform.[28] These results from studies utilizing optical spectroscopy are in good agreement with our theoretical calculations.

However, our results on the effects hydrogen bonding in formamide are not consistent with the ionic model proposed by Fillaux.[5] According to the ionic model, the fundamental N−H stretching frequency should be about ∼1575 cm^{-1}. Our assignments place the N−H stretching frequency at about 3300 cm^{-1}, which is inconsistent with the ionic model. In addition, the low-temperature Raman data show an intense and sharp band at 3124 cm^{-1}, and no Raman band about 1575 cm^{-1} was observed.[25] This demonstrates conclusively that the fundamental N−H stretching frequency is about 3100−3200 cm^{-1}. The Raman data are in better agreement with our theoretical models than the ionic model. The broad INS signal in the region around 1575 cm^{-1} in the INS spectrum of formamide can be explained on the basis of a conventional interpretation of the inelastic neutron scattering. The force field model used by Fillaux et al. is based on a single-molecule approach where the force constants for the various motions were refined from the experimental data. The approach taken in this paper is a first-principles method, and given the good agreement between the theory and the optical and neutron spectra, the conclusion must be that the ionic model for the bonding in simple amides is incorrect. This incorrect assignment of the N−H stretch by Fillaux et al. is based on the intensity of the mode at 1575 cm^{-1}, and it is likely that the empirical force field model does not correctly estimate the vibrational amplitudes.

Moreover, the main feature of the ionic model is that the hydrogen bonded hydrogen atoms are not formally bonded to the nitrogen atoms. Instead, there is a dynamical proton exchange between the amidic (···OCNH···) and imidolic (···HOCN···) forms. If this is true for the case of formamide, the time-averaged N−H bond length in solid formamide must exceed substantially the value for an isolated N−H bond. The neutron diffraction study of crystalline formamide shows that the N−H bond length in the crystal is only very slightly longer than is the case for an ordinary N−H bond.[17] Consequently, the ionic model is definitely not applicable in the case of solid formamide.

Although the effects of hydrogen bonding on the N−H vibrational frequencies are clearly observed in our study, some difficulties remain when modeling a real crystal with a small cluster. First, not all the N-hydrogen atoms are hydrogen bonded to the nearest oxygen atoms. Two different types of N-hydrogen atoms (H-bonded and non-H-bonded) are present, and they give rise to different N−H vibrational frequencies. Naturally, all the N-hydrogen in a real crystal are hydrogen bonded. Therefore, some strong extra bands exist in the simulated INS spectra due to the "free" N-hydrogen. Also the model lacks the interaction between the crystal unit planes. As mainly the NH_2 out-of-plane wagging frequency is affected by the H-bonding, we can expect a significant effect from such an interplanar interaction. Nevertheless, as far as the main spectral features and the normal mode assignments are concerned, the small cluster modeling seems to be sufficient. The ab initio approach used in this study could be improved either by an increase in the size of the cluster, or by solving the Schroedinger equation under periodic boundary conditions.

The simple concept that "the stronger the bond the higher the stretching frequency" can be demonstrated for the case of hydrogen bonding in solid formamide. Within the FA4 cluster, for example, the N−H and C═O stretching frequencies decrease by ∼2−5% (with an increase in their bond lengths), when compared to an isolated FA molecule. On the other hand, the NH_2 torsion and wagging frequencies increase by ∼25% and ∼300%, respectively. The agreement between the simulated and experimental spectra in the NH_2 torsion mode region is encouraging, as shown in Figures 3 and 4. However, due to the imperfection of the models (insufficient H-bonds), the true NH_2 wagging frequencies should even be higher. The NH_2 wagging frequency for the inner pairs of FA4 is slightly higher than that for the outer pairs. This is mainly due to the different

H-bonds connected with the inner (cyclic H-bonds) and outer (zigzag H-bonds) pairs. The inner pairs describe the crystal environment better than the outer pairs. Following this trend, the true NH_2 wagging frequencies may actually be around 800−900 cm^{-1} (about 600% increase from NH_2 wagging frequency for the monomer). Also, the true vibrational amplitudes for these NH_2 wagging motions, with every N−H atom pair being H-bonded, will be much smaller than that for the "free" N−H atoms. The INS intensities for these NH_2 wagging modes are therefore overestimated in the calculations. The INS signals for the NH_2 wagging modes may be hidden inside the experimental INS bands at 800−900 cm^{-1}. This is consistent with the low-temperature IR data, which indicates a NH_2 wagging frequency of 841 cm^{-1}.[25]

Conclusion

Hydrogen bonding has a significant effect on the INS intensities and vibrational frequencies of crystalline formamide. Ab initio harmonic force field calculations using the DFT method and small cluster models are reasonably successful in reproducing the experimental INS spectra. The results of this study are inconsistent with the previously proposed interpretation of the INS spectra of solid *N*-methylacetamide based on a double well (anharmonic) ionic model. The solid formamide spectrum can be interpreted using conventional ab initio modeling of the harmonic force field (or with an anharmonic perturbational part) if calculated at a reasonably high level for a carefully chosen model system. Further improvements in the agreement between the theoretical calculations and the experimental data are likely if larger clusters are used, to minimize the cluster surface effects. An even better solution would be to use ab initio codes incorporating periodic boundary conditions, and although such codes are being developed, they are not yet able to provide the necessary parameters for a prediction of INS spectra.

Acknowledgment. We would like to thank Mr. Paul Rickert for his help on the NMR measurement of the N-deuterated formamide. This work has benefited from the use of the Intense Pulsed Neutron Source at Argonne National Laboratory. This facility is funded by the U.S. Department of Energy, BES-Materials Science, under Contract W-31-109-Eng-38.

References and Notes

(1) Jeffery, G. A.; Saenger, W. In *Hydrogen Bonding in Biological Structures*; Springer-Verlag: Berlin, 1991.

(2) Surewicz, W. K.; Mantsch, H. H. *Biochim. Biophys. Acta* **1988**, *952*, 115 and references therein.

(3) Miyazawa, T.; Shimanoushi, S.; Mizushima, S. *J. Chem. Phys.* **1958**, *29*, 611.

(4) Parker, F. S. *Applications of Infrared and Raman Spectroscopy in Biochemistry*; Plenum: New York, 1983. Surewicz, W. K.; Mantsch, H. H.; Chapman, D. *Biochemistry* **1993**, *32*, 389.

(5) Fillaux, F.; Fontaine, J. P.; Baron, M.-H.; Kearley, G. J.; Tomkinson, J. *Chem. Phys.* **1993**, *176*, 249. Kearley, G. J.; Fillaux, F.; Baron, M.-H.; Bennington, S.; Tomkinson, J. *Science* **1994**, *264*, 1285.

(6) Tomkinson, J. *Spectrochim. Acta* **1992**, *48A*, 329.

(7) Lautié, A.; Froment, F.; Novak, A. *Spectrosc. Lett.* **1976**, *9*, 289.

(8) Florián, J.; Leszczynski, J.; Johnson, B. G. *J. Mol. Struct.* **1995**, *349*, 421.

(9) Lifson, S.; Hagler, A. T.; Dauber, P. *J. Am. Chem. Soc.* **1979**, *101*, 5111. Jorgensen, W. L.; Swensen, C. J. *J. Am. Chem. Soc.* **1985**, *107*, 1489.

(10) Lee, C.; Yang, W.; Parr, R. G. *Phys. Rev. B* **1988**, *37*, 785.

(11) Becke, A. D. *J. Chem. Phys.* **1993**, *98*, 5648. Becke, A. D. In *The Challenge of d and f electrons*; Salahub, D. R., Zerner, M. C., Eds.; American Chemical Society: Washington, DC, 1989.

(12) Bour, P.; Tam, C. N.; Shaharuzzaman, M.; Chickos, J. S.; Keiderling, T. A. *J. Phys. Chem.* **1996**, *100*, 15041. Tam, C. N.; Bour, P.; Keiderling, T. A. *J. Am. Chem. Soc.* **1996**, *118*, 10285.

(13) Fan, L.; Ziegler, T. *J. Chem. Phys.* **1992**, *96*, 9005. Berces, A.; Ziegler, T. *J. Chem. Phys.* **1993**, *98*, 4793.

(14) Handy, N. C.; Murray, C. W.; Amos, R. D. *J. Phys. Chem.* **1993**, *97*, 4392.

(15) Florián, J.; Johnson, B. G. *J. Phys. Chem.* **1994**, *98*, 3681.

(16) Frisch, M. J. *GAUSSIAN 94*; Gaussian Inc.: Pittsburgh, PA, 1994.

(17) Torrie, B. H.; O'Donovan, C.; Powell, B. M. *Mol. Phys.* **1994**, *82*, 643.

(18) Bour, P.; Bednarova, L.; Sopkova, J.; Malon, P.; Keiderling, T. A. *J. Comput. Chem.* **1997**, *18*, 649.

(19) Florián, J. *J. Phys. Chem.* **1993**, *97*, 10649. Kearley, G. J. *J. Chem. Soc., Faraday Trans. 2* **1986**, *82*, 41. Kearley, G. J. *Nucl. Instrum. Methods* **1995**, *A354*, 53. Tomkinson, J.; Warner, M.; Taylor, A. D. *Mol. Phys.* **1984**, *51*, 381.

(20) Blundel, T. L.; Johnson, L. N. *Protein Crystallography*; Academic Press: London, 1993; p 468.

(21) Bour, P. *J. Phys. Chem.* **1994**, *98*, 8862.

(22) Stevens, E. D. *Acta Crystallogr.* **1978**, *341*, 544.

(23) Kitano, M.; Kuchitsu, K. *Bull. Chem. Soc. Jpn.* **1974**, *47*, 67.

(24) Suhai, S. *J. Phys. Chem.* **1996**, *100*, 3950.

(25) Torrie, B. H.; Brown, B. A. *J. Raman Spectrosc.* **1993**, *25*, 183.

(26) Bour, P.; Bednarova, L. *J. Phys. Chem.* **1995**, *99*, 5961.

(27) Fillaux, F.; Baron, M.-H. *Chem. Phys.* **1981**, *62*, 275.

(28) Tam, C. N. Ph.D. Thesis; The University of Illinois at Chicago, 1995.